

inferred final mass ratio is $M_{\text{BH}}/M_* \sim 1/50$. This growth can only occur if star formation continues for a relatively long period (≥ 1 Gy) and at a high rate ($>50 M_\odot \text{ year}^{-1}$). This would require the presence of a substantial reservoir, or the accretion, of cold gas, which, however, could not increase the SMBH mass by much. Finally, in the most extreme scenario, the star formation shuts down almost immediately (i.e., due to the AGN-driven outflow), and the system remains “frozen” at $M_{\text{BH}}/M_* \sim 1/10$ throughout cosmic time. If the SMBH does indeed grow further (i.e., beyond $10^{10} M_\odot$), this would imply yet higher M_{BH}/M_* . Thus, the inferred final BH-to-stellar mass ratio for CID-947 is, in the most extreme scenarios, about $M_{\text{BH}}/M_* \sim 1/100$, and probably much higher (see Fig. 2).

CID-947 therefore represents a progenitor of the most extreme, high-mass systems in the local universe, like NGC 1277. Such systems are not detected in large numbers, perhaps due to observational selection biases. The above considerations indicate that the local relics of systems like CID-947 are galaxies with at least $M_* \sim 5 \times 10^{11} M_\odot$. Such systems are predominantly quiescent (i.e., with low star-formation rates, $\text{SFR} \ll 1 M_\odot \text{ year}^{-1}$) and relatively rare in the local universe, with typical number densities on the order of $\sim 10^{-5} \text{ Mpc}^{-3}$ (26). We conclude that CID-947 provides direct evidence that at least some of the most massive BHs, with $M_{\text{BH}} \geq 10^{10} M_\odot$, already in place just 2 Gy after the Big Bang, did not shut down star formation in their host galaxies. The host galaxies may experience appreciable mass growth in later epochs, without much further black hole growth, resulting in very high stellar masses but still relatively high M_{BH}/M_* . Lower-mass systems may follow markedly different coevolutionary paths. However, systems with M_{BH}/M_* as high as in CID-947 may be not as rare as previously thought, as they can be consistently observed among populations with number densities on the order of $\sim 10^{-5} \text{ Mpc}^{-3}$, both at $z > 3$ and in the local universe, and not just among the rarest, most luminous quasars.

REFERENCES AND NOTES

1. L. Ferrarese, D. Merritt, *Astrophys. J.* **539**, L9–L12 (2000).
2. K. Gebhardt et al., *Astrophys. J.* **539**, L13–L16 (2000).
3. X. Z. Zheng et al., *Astrophys. J.* **707**, 1566–1577 (2009).
4. J. Kormendy, L. C. Ho, *Annu. Rev. Astron. Astrophys.* **51**, 511–653 (2013).
5. A. C. Fabian, *Annu. Rev. Astron. Astrophys.* **50**, 455–489 (2012).
6. A. Merloni et al., *Astrophys. J.* **708**, 137–157 (2010).
7. R. Decarli et al., *Mon. Not. R. Astron. Soc.* **402**, 2453–2461 (2010).
8. V. N. Bennert, M. W. Auger, T. Treu, J.-H. Woo, M. A. Malkan, *Astrophys. J.* **742**, 107 (2011).
9. O. Shemmer et al., *Astrophys. J.* **614**, 547–557 (2004).
10. H. Netzer, P. Lira, B. Trakhtenbrot, O. Shemmer, I. Cury, *Astrophys. J.* **671**, 1256–1263 (2007).
11. G. De Rosa et al., *Astrophys. J.* **739**, 56 (2011).
12. B. Trakhtenbrot, H. Netzer, P. Lira, O. Shemmer, *Astrophys. J.* **730**, 7 (2011).
13. D. Masters et al., *Astrophys. J.* **755**, 169 (2012).
14. N. Z. Scoville et al., *Astrophys. J. Suppl. Ser.* **172**, 1–8 (2007).
15. F. Civano et al., *Astrophys. J.* **741**, 91 (2011).
16. Data and methods, supplementary text, figures and tables are available on Science Online.
17. Y. Shen, *Bull. Astron. Soc. Ind.* **41**, 61 (2013).
18. N. J. McConnell et al., *Astrophys. J.* **756**, 179 (2012).
19. M. Volonteri, *Astron. Astrophys. Rev.* **18**, 279–315 (2010).
20. A. Bongiorno et al., *Mon. Not. R. Astron. Soc.* **427**, 3103–3133 (2012).

21. O. Ilbert et al., *Astron. Astrophys.* **556**, A55 (2013).
22. J. S. Speagle, C. L. Steinhardt, P. L. Capak, J. D. Silverman, *Astrophys. J. Suppl. Ser.* **214**, 15 (2014).
23. N. Häring, H. Rix, *Astrophys. J.* **604**, L89 (2004).
24. R. C. E. van den Bosch et al., *Nature* **491**, 729–731 (2012).
25. E. Emsellem, *Mon. Not. R. Astron. Soc.* **433**, 1862–1870 (2013).
26. I. K. Baldry et al., *Mon. Not. R. Astron. Soc.* **421**, 621 (2012).
27. J. L. Walsh, A. J. Barth, L. C. Ho, M. Sarzi, *Astrophys. J.* **770**, 86 (2013).
28. K. Gebhardt et al., *Astrophys. J.* **729**, 119 (2011).
29. C. Y. Peng et al., *Astrophys. J.* **649**, 616 (2006).
30. R. J. McLure, M. J. Jarvis, T. A. Targett, J. S. Dunlop, P. N. Best, *Mon. Not. R. Astron. Soc.* **368**, 1395–1403 (2006).

ACKNOWLEDGMENTS

The new MOSFIRE data presented herein were obtained at the W. M. Keck Observatory, which is operated as a scientific partnership among the California Institute of Technology, the University of California, and the National Aeronautics and Space Administration. The Observatory was made possible by the generous financial support of the W. M. Keck Foundation. We thank M. Kassis and the rest of the staff at the W. M. Keck observatories at Waimea, HI, for their support during the observing run. We recognize and acknowledge the very significant cultural role and reverence that the summit of Mauna Kea has always had within the indigenous Hawaiian community. We are most

fortunate to have the opportunity to conduct observations from this mountain. Some of the analysis presented here is based on data products from observations made with European Southern Observatory (ESO) Telescopes at the La Silla Paranal Observatory under ESO program ID 179.A-2005 and on data products produced by TERAPIX and the Cambridge Astronomy Survey Unit on behalf of the UltraVISTA consortium. We are grateful to A. Faisst and M. Onodera for their assistance with the acquisition and reduction of the MOSFIRE data. We thank S. Tacchella, J. Woo, and W. Hartley for their assistance with some of the evolutionary calculations. K.S. gratefully acknowledges support from Swiss National Science Foundation Professorship grant PP00P2 138979/1. F.C. acknowledges financial support by the NASA grant G03-14150C. M.E. acknowledges financial support by the NASA Chandra grant G02-13127X. B.T. is a Zwicky Fellow at the ETH Zurich.

SUPPLEMENTARY MATERIALS

www.sciencemag.org/content/349/6244/168/suppl/DC1
Data, Methods, and Supplementary Text S1 to S4
Figs. S1 to S4
Table S1
References (31–81)

10 December 2014; accepted 29 May 2015
10.1126/science.aaa4506

ANIMAL PHYSIOLOGY

Exceptionally low daily energy expenditure in the bamboo-eating giant panda

Yonggang Nie,^{1*} John R. Speakman,^{2,3*} Qi Wu,^{1*} Chenglin Zhang,⁴ Yibo Hu,¹ Maohua Xia,⁴ Li Yan,¹ Catherine Hambly,³ Lu Wang,² Wei Wei,¹ Jinguo Zhang,⁴ Fuwen Wei^{1†}

The carnivorous giant panda has a specialized bamboo diet, to which its alimentary tract is poorly adapted. Measurements of daily energy expenditure across five captive and three wild pandas averaged 5.2 megajoules (MJ)/day, only 37.7% of the predicted value (13.8 MJ/day). For the wild pandas, the mean was 6.2 MJ/day, or 45% of the mammalian expectation. Pandas achieve this exceptionally low expenditure in part by reduced sizes of several vital organs and low physical activity. In addition, circulating levels of thyroid hormones thyroxine (T_4) and triiodothyronine (T_3) averaged 46.9 and 64%, respectively, of the levels expected for a eutherian mammal of comparable size. A giant panda–unique mutation in the *DUOX2* gene, critical for thyroid hormone synthesis, might explain these low thyroid hormone levels. A combination of morphological, behavioral, physiological, and genetic adaptations, leading to low energy expenditure, likely enables giant pandas to survive on a bamboo diet.

The giant panda (*Ailuropoda melanoleuca*) is an enigmatic, critically endangered bear endemic to China. Its diet is made up almost exclusively of bamboo, but it retains a short carnivorous alimentary tract and, consequently, has very low digestive efficiency (1–3). Therefore, the giant panda must feed for a large part of each day and consume large quantities of food relative to its body mass (1, 4). This has led to speculation that giant pandas must also have low metabolic rates to achieve a daily energy balance (1). We report the first measurements of daily energy expenditure (DEE) of captive and free-living giant pandas, measured using the doubly labeled water (DLW) method (5) (see supplementary materials and methods). We validated these measurements using estimates of

net energy assimilation and matched them with morphological, behavioral, physiological, and genetic data. We measured the DEE of five captive and three free-living pandas (supplementary text S1, tables S1.3 and S1.4). Across the captive individuals, the body mass averaged 91.1 kg and DEE averaged 4.6 ± 0.9 MJ/day (\pm SEM) ($n = 5$ animals). In the wild, the equivalent values were

¹Key Laboratory of Animal Ecology and Conservation Biology, Institute of Zoology, Chinese Academy of Sciences, Beijing, China. ²State Key Laboratory of Molecular Developmental Biology, Institute of Genetics and Developmental Biology, Chinese Academy of Sciences, Beijing, China. ³Institute of Biological and Environmental Sciences, University of Aberdeen, Aberdeen, Scotland, UK. ⁴Beijing Key Laboratory of Captive Wildlife Technologies, Beijing Zoo, Beijing, China.

*These authors contributed equally to this work.
†Corresponding author. E-mail: weifw@ioz.ac.cn

92.6 kg and 6.2 ± 1.5 MJ/day ($n = 3$ animals). There was a significant effect of body mass on DEE (regression $P < 0.001$; coefficient of determination $r^2 = 83.8\%$) but no significant difference between captive and wild animals ($P = 0.081$) (Fig. 1A). The pooled estimate was 5.2 ± 0.7 MJ/day ($n = 8$ animals). We validated these estimates by comparing the DEE by DLW to the net energy assimilation (NEA) estimated from individual measures of assimilation efficiency, multiplied by the daily fecal production, measured in three captive pandas almost daily for 11 months ($n = 961$ animal days). Assimilation efficiency varied between 11.1 and 20.5% (supplementary text S2), comparable to previous estimates in captive pandas (7.4 to 38.9%) (2, 6, 7). Daily NEA (megajoules per day) varied over the year, being higher in the winter months (Fig. 1B). Consequently, there was a significant negative relationship between NEA and the average daily shade temperature (Fig. 1C) [regression: $F_{1,37} = 197.9$, $P < 0.001$]. Across all measurements, the average NEA was 7.0 ± 2.1 MJ/day (\pm SD). A prior estimate of NEA for giant pandas in captivity was 4.2 MJ/day (7), slightly lower than our measured value, probably because it was made at a higher ambient temperature. Excepting a single value, the DEE data were within the standard deviations of the NEA data. We used the fitted

equation between NEA and ambient temperature to predict the expected NEA on the days the DLW method was used. The measured DEE averaged $77.0 \pm 7.3\%$ (\pm SD) of the predicted NEA (absolute mean discrepancy 1.6 ± 0.49 MJ/day). This discrepancy exists because NEA values do not account for energy in urine, which is high because of the role of panda urine in scent marking (8). Combining the water turnover from the DLW estimates with the water loss in feces indicated that pandas may produce maximally 5.0 liters of urine daily (supplementary text S2). Linking this estimate with direct measurements of urine solid matter and energy content suggests that pandas may maximally eliminate 2.1 MJ/day in urine, not significantly different from the mean discrepancy between the NEA and DEE estimates (t test: $t = 2.02$, $P = 0.136$).

The DEE by DLW was only 37.7% of the expectation (45% for the field data) for a terrestrial mammal on the basis of body mass (Fig. 1D) (9). These values are substantially lower than those for other mammals considered to have low DEE, such as the koala (*Phascolarctos cinereus*) at 69% and the echidna (*Tachyglossus aculeatus*) at 66% of the expected value. Additionally, for the pooled DLW estimate, our values were almost equal to that of the three-toed sloth (*Bradypus variegatus*)

at 36% of the prediction. The lowest reported primate DEE is for the ring-tailed lemur (*Lemur catta*) at 52% of expected (10). Only two other mammals have relative DEE values that are considerably lower than those of the giant panda: the Australian rock rat (*Zygomys argurus*) (21% of the predicted level) (11) and the desert golden mole (*Eremitalpa namibensis*) (26% of expected) (12). However, it is unclear whether these small animals were using torpor during the measurements. Otherwise, the measurements for the giant panda are among the lowest, relative to body mass, ever made for a nontorpid mammal. In fact, DEE in the giant panda (and sloth) is closer to the expectations for a 92-kg reptile (4.9 MJ/day) (13) than for a terrestrial mammal.

Animals may achieve low rates of metabolism via behavioral, morphological, and physiological adaptations. Low metabolic rates may be achieved by relaxing homeothermy (14). However, giant panda body temperatures indicate that they do not engage in either daily torpor or hibernation (15). Presumably, giant pandas can sustain a high body temperature, despite their low DEE, because they have a deep pelage able to trap their meager body heat (1). Supporting this hypothesis, measurements of lateral surface temperatures of giant pandas are significantly lower than those of

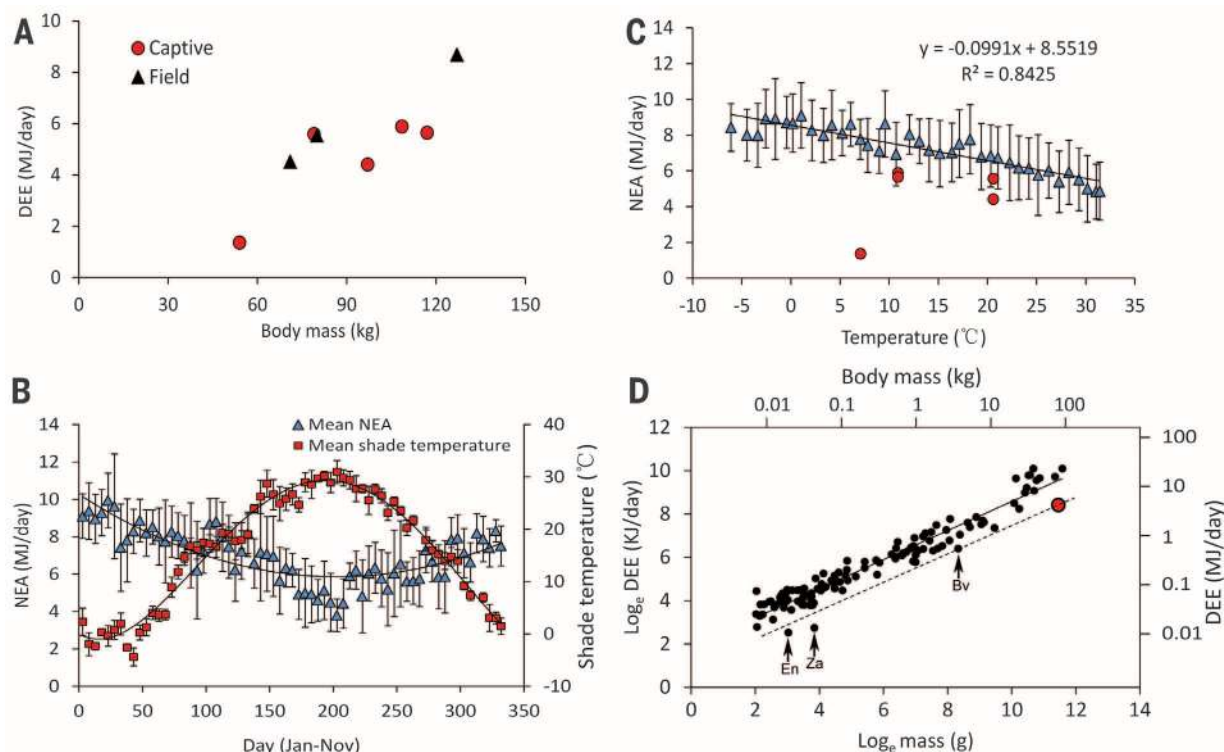


Fig. 1. Daily energy demands of the giant panda. (A) Daily energy expenditure (DEE) (megajoules per day) using the DLW method for eight pandas in relation to body mass (kilograms). Captive animals ($n = 5$) are represented by red circles and wild animals ($n = 3$) by black triangles. (B) Net energy assimilation (NEA) (megajoules per day) averaged across three captive pandas estimated from assimilation efficiency and daily fecal production and plotted against day of year (1 January = 1). Air temperatures (red squares) are also shown (mean \pm SD). (C) NEA (megajoules per day) plotted against ambient temperature (blue triangles with SD) and DEE (megajoules per day) of five

captive individuals by DLW (red circles). (D) DEE by DLW of terrestrial mammals [\log_e field metabolic rate (FMR) (kilojoules per day)] plotted against body mass [\log_e mass (grams)]. Each point represents a different species [data from (9) and (10)]. The solid line is the equation \log_e (FMR in kilojoules per day) = $1.871 + 0.67[\log_e$ mass (grams)] [from (9)]. The giant panda is represented by the red data point. The dotted line is equal to 37% of the prediction equation. Some other animals with low metabolism are indicated. Bv, *B. variegatus* (three-toed sloth); En, *E. namibensis* (desert golden mole); Za, *Z. argurus* (Australian rock rat).

zebras (*Equus quagga*), dairy cattle (*Bos taurus*), and domestic dogs (*Canis familiaris*) (Fig. 2).

Animals may also reduce DEE by minimizing the time spent in and intensity of physical activity. We measured the activity of captive pandas by direct observation and in the wild using GPS loggers and direct observation. In captivity, the

animals spent 33% of their time being physically active; in the wild, 49% of their time was devoted to physical activity. These findings are similar to those reported previously (16). Pandas in the wild were more active than those in captivity (t test: $t = -3.93$, $P = 0.017$) (Fig. 3A). Compared with other bears, pandas had lower levels of activity (1, 17).

In the wild, both the foraging movement speed (15.5 m/hour) and the mean movement speed (26.9 m/hour) were very low (Fig. 3B).

For larger terrestrial mammals, the dominant component of the daily energy budget is the resting metabolic rate (9). Resting metabolism is derived from the summed metabolic

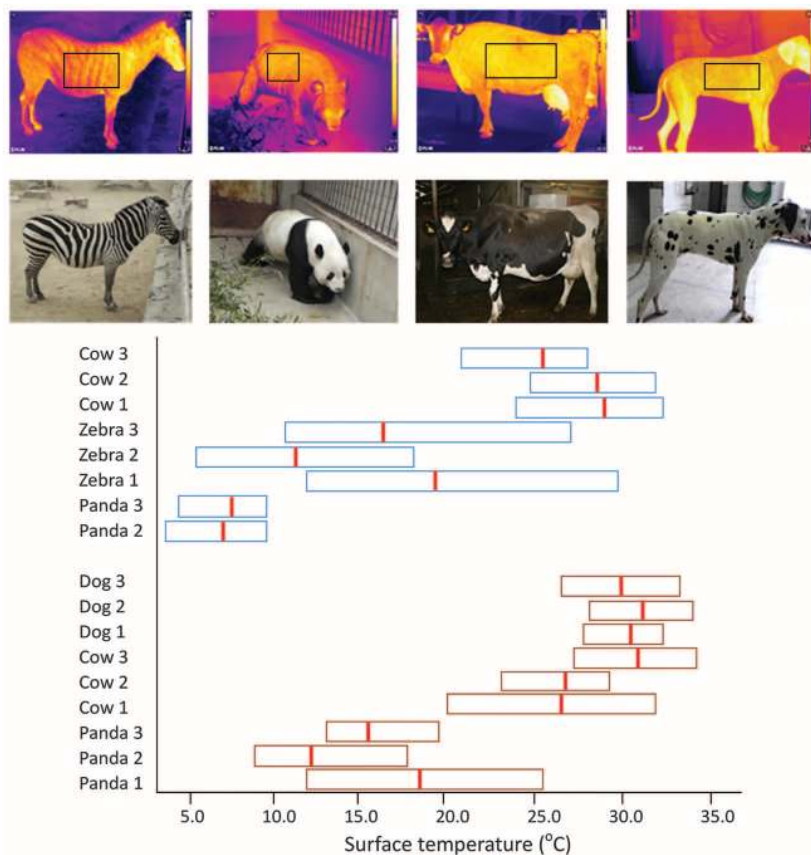


Fig. 2. Surface temperatures of giant pandas, zebras, Holstein cows, and Dalmatian dogs at ambient air temperatures of ~4°C (blue boxes) and 10°C (brown boxes). The pictures show representative thermal images (top) and normal images (bottom). The plot underneath shows the analysis of lateral surface temperatures. Boxes represent the range of surface temperatures (minimum to maximum). Mean values are denoted by the red bars. (See supplementary materials for more details.)

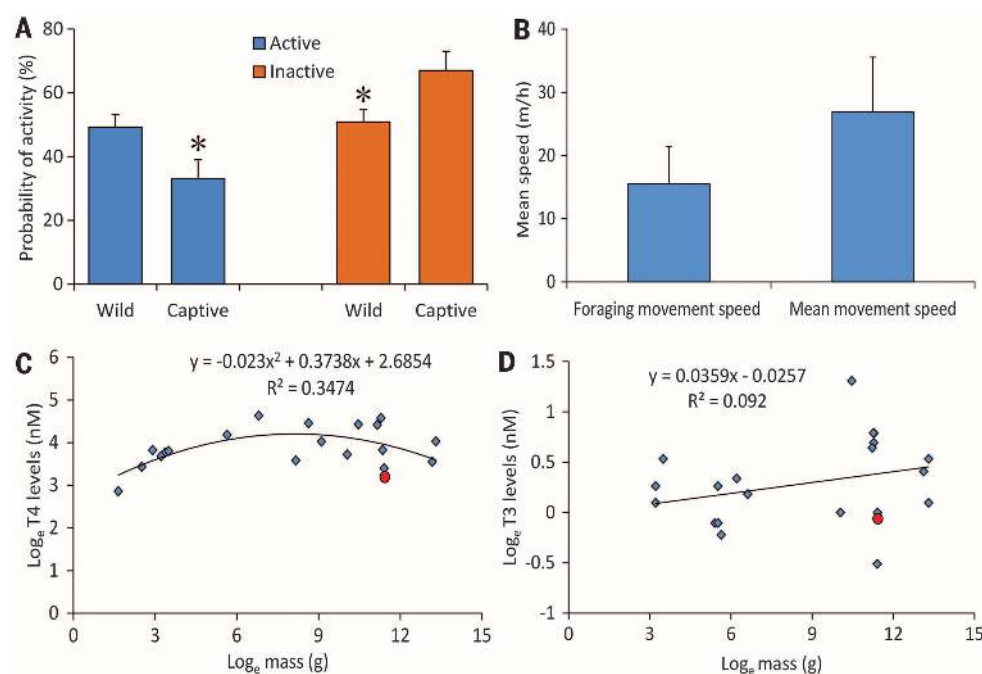


Fig. 3. Physical activity and thyroid hormone levels. (A) Physical activity levels in wild and captive pandas (mean \pm SD). Asterisks indicate $P < 0.05$ (t test). (B) Movement speed when foraging and mean movement speed (mean \pm SD) over the whole year in wild pandas. Thyroid hormone levels for (C) T₄ and (D) T₃ in eutherian mammals (blue diamonds) [data from (28)]. Each data point represents a different species. The fitted curves show the best-fit polynomial relationships with the associated equations in the respective panels. The giant panda is represented by the red data points.

rates of the body components (18). Some organs such as the liver, brain, kidneys, and heart contribute disproportionately to the total (19). We used literature autopsy data to assess whether pandas have relatively small organ sizes (supplementary text S3, table S3). Giant pandas have relatively small brains, livers, and kidneys (respectively, 82.5, 62.8, and 74.5% of expectation) compared with other eutherian mammals. These reduced organ sizes probably contribute to their low energy demands. Resting metabolic rate is also strongly influenced by several hormones, particularly the thyroid hormones (20) thyroxine (T_4) and triiodothyronine (T_3). In the same captive animals in which we measured DEE, total T_4 averaged 24.44 ± 1.17 nM (\pm SEM), and total T_3 averaged 0.94 ± 0.05 nM, similar to previous giant panda measurements (21). The T_4 level was 46.9%, and T_3 64.0%, of the expectation for a eutherian mammal of the same body mass (Fig. 3, C and D). These measurements were lower than in hibernating black bears (*Ursus americanus*) (22). In Fig. 3D, the data point lower than that for the panda is representative of the gray seal (*Halichoerus grypus*); gray seals are believed to have low T_3 levels to facilitate metabolic suppression during diving. Pandas clearly have low levels of both T_4 and T_3 , which may be instrumental in their exceptionally low metabolism.

We compared the panda genome with the genomes of five other carnivorans, mouse, and human. We did not find any notable mutations in

the promoter regions and exons or introns of the 182 genes listed in the Kyoto Encyclopedia of Genes and Genomes as linked to the thyroid hormone synthesis and thyroid signaling pathways, with one exception. A unique variation was found in the dual oxidase 2 (*DUOX2*) gene in the panda, which is homologous to the *DUOX2* gene in humans. *DUOX2* encodes a transmembrane protein that catalyzes the conversion of water to hydrogen peroxide, which is used in the final step of T_4 and T_3 synthesis. The giant panda *DUOX2* gene contains a single substitution of C to T in the 16th exon, which causes a premature stop codon (TGA) (Fig. 4). This mutation is also observed in transcriptome data, suggesting that the transcript of *DUOX2* would not be translated into a complete protein. In humans and mice, loss-of-function mutations in *DUOX2* lead to hypothyroidism (23–25).

Although the metabolic rates of the giant panda are exceptionally low, we do not suggest that they are entirely separate from other eutherian mammals. Other folivorous animals, like the three-toed sloth, also have very low DEEs, and this is probably true of several other species, such as the frugivorous binturong (*Arctictis binturong*) and the folivorous red panda (*Ailurus fulgens*), both of which have very low basal rates of metabolism (26). Rather, the giant panda represents one end of a spectrum of metabolic rates where the dominant ultimate factors may be the quality and quantity of the food they exploit (27).

Giant pandas have exceptionally low DEE, which may facilitate survival on their diet of bamboo. A suite of behavioral, morphological, and physiological factors—including low physical activity levels and reduced sizes of some high metabolism organs—probably contribute to the low energy expenditure. Additionally, levels of the thyroid hormones are about half of the expected amounts. This may be linked, in part, to mutations in the panda genome in the *DUOX2* gene, which catalyzes a key step in T_4 and T_3 synthesis.

REFERENCES AND NOTES

- G. B. Schaller, J. C. Hu, W. S. Pan, J. Zhu, *The Giant Panda of Wolong* (Univ. of Chicago Press, Chicago, 1985).
- E. S. Dierenfeld, H. F. Hintz, J. B. Robertson, P. J. Van Soest, O. T. Oftedal, *J. Nutr.* **112**, 636–641 (1982).
- F. Wei et al., *Mol. Biol. Evol.* **32**, 4–12 (2015).
- W. S. Pan, Z. Lv, X. J. Zhu, D. J. Wang, H. Wang, Y. Long, D. L. Fu, X. Zhou, *A Chance for Lasting Survival*, W. J. McShea, R. B. Harris, D. L. Garshelis, D. J. Wang, Eds. (Smithsonian Institution Scholarly Press, Washington, DC, 2014).
- P. J. Butler, J. A. Green, I. L. Boyd, J. R. Speakman, *Funct. Ecol.* **18**, 168–183 (2004).
- S. A. Mainka, G. Zhao, M. Li, *J. Zoo Wildl. Med.* **20**, 39–44 (1989).
- T. G. Finley et al., *Zoo Biol.* **30**, 121–133 (2011).
- Y. G. Nie et al., *Anim. Behav.* **84**, 39–44 (2012).
- J. R. Speakman, E. Król, *J. Anim. Ecol.* **79**, 726–746 (2010).
- H. Pontzer et al., *Proc. Natl. Acad. Sci. U.S.A.* **111**, 1433–1437 (2014).
- S. D. Bradshaw, K. D. Morris, C. R. Dickman, P. C. Withers, D. Murphy, *Aust. J. Zool.* **42**, 29–41 (1994).
- M. Scantlebury, M. K. Oosthuizen, J. R. Speakman, C. R. Jackson, N. C. Bennett, *Physiol. Behav.* **84**, 739–745 (2005).
- K. A. Nagy, I. A. Girard, T. K. Brown, *Annu. Rev. Nutr.* **19**, 247–277 (1999).
- F. Geiser, *Annu. Rev. Physiol.* **66**, 239–274 (2004).
- Y. C. Cheng, Y. H. Cheng, *Chin. J. Wildlife* **4**, 46–47 (1983).
- M. A. Owen, N. M. Czekala, R. R. Swaisgood, K. Steinman, D. G. Lindburg, *Ursus* **16**, 208–221 (2005).
- A. G. MacHutchon, *Ursus* **12**, 189–198 (2001).
- Z. Wang, T. P. O'Connor, S. Heshka, S. B. Heymsfield, *J. Nutr.* **131**, 2967–2970 (2001).
- M. Elia, in *1st Clintec International Horizons Conference on Energy Metabolism: Tissue Determinants and Cellular Corollaries*, J. M. Kinney, H. N. Tucker, Eds. (Raven, New York, 1992), pp. 19–59.
- J. E. Silva, *Physiol. Rev.* **86**, 435–464 (2006).
- Z. H. Zhang, F. W. Wei, *Giant Panda Ex-situ Conservation: Theory and Practice* (Sciences Press, Beijing, 2006).
- T. E. Tomasi, E. C. Hellgren, T. J. Tucker, *Gen. Comp. Endocrinol.* **109**, 192–199 (1998).
- J. C. Moreno et al., *N. Engl. J. Med.* **347**, 95–102 (2002).
- N. Pfarr et al., *Clin. Endocrinol.* **65**, 810–815 (2006).
- K. R. Johnson et al., *Mol. Endocrinol.* **21**, 1593–1602 (2007).
- B. K. McNab, *Acta Zool. Sinica* **51**, 535–545 (2005).
- B. K. McNab, *Extreme Measures: The Ecological Energetics of Birds and Mammals* (Univ. of Chicago Press, Chicago, 2012).
- A. J. Hulbert, *Biol. Rev. Camb. Philos. Soc.* **75**, 519–631 (2000).
- W. J. Kent et al., *Genome Res.* **12**, 996–1006 (2002).

ACKNOWLEDGMENTS

We thank X. Wang, Y. Jin, W. Zhou, T. Pu, X. Wang, L. Shan, S. Ma, W. Du, Z. Tan, M. Wang, X. Zheng, H. Han, D. Wang, and T. Ma for help with the data collection and P. Thompson for technical assistance with the isotope analysis. We also thank the Foping Nature Reserve and Beijing Zoo for their assistance on this study. This work was supported jointly and equally by the Key Project of National Natural Science Foundation of China (grant 31230011) and the Strategic Priority Research Program of the Chinese Academy of Sciences (grant XDB13030000). The thermal image camera used for the dairy cow images was on loan from the UK Engineering and Physical Sciences Research Council equipment loan pool. The physiological and other data are presented in the supplementary materials. The genetic data have been deposited in the National Center for Biotechnology Information database with accession number KT000656.

SUPPLEMENTARY MATERIALS

www.sciencemag.org/content/349/6244/171/suppl/DC1

Materials and Methods

Supplementary Text

Fig. S1

Tables S1 to S3

References (30–51)

31 March 2015; accepted 3 June 2015

10.1126/science.aab2413

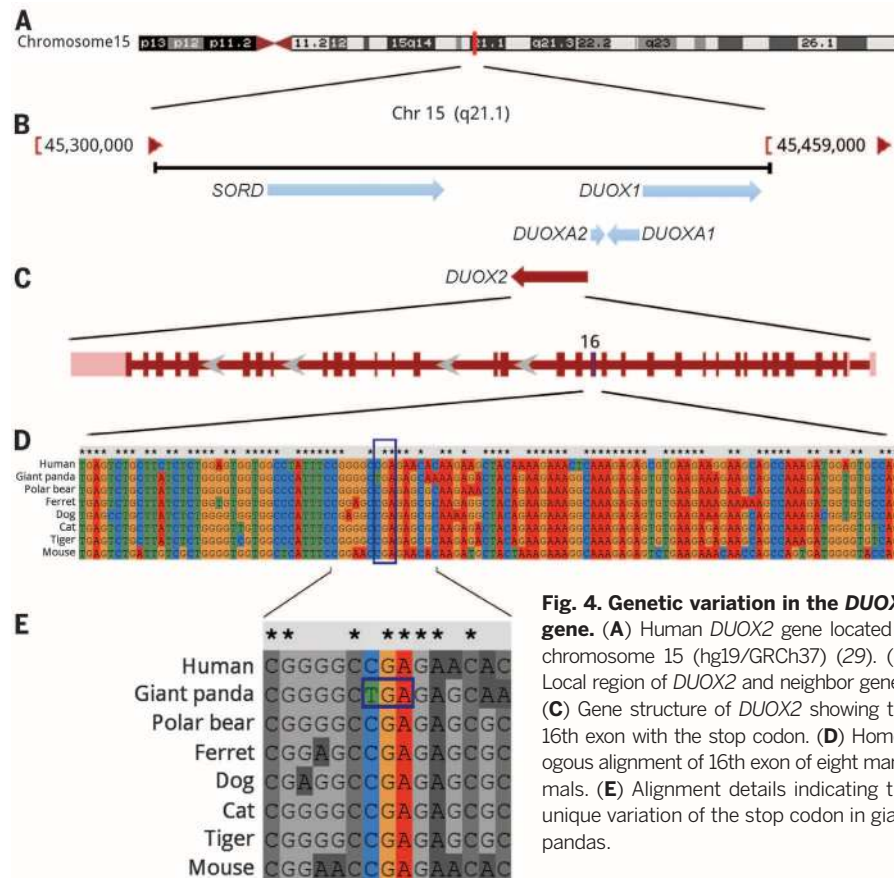


Fig. 4. Genetic variation in the *DUOX2* gene. (A) Human *DUOX2* gene located in chromosome 15 (hg19/GRCh37) (29). (B) Local region of *DUOX2* and neighbor genes. (C) Gene structure of *DUOX2* showing the 16th exon with the stop codon. (D) Homologous alignment of 16th exon of eight mammals. (E) Alignment details indicating the unique variation of the stop codon in giant pandas.

This copy is for your personal, non-commercial use only.

If you wish to distribute this article to others, you can order high-quality copies for your colleagues, clients, or customers by [clicking here](#).

Permission to republish or repurpose articles or portions of articles can be obtained by following the guidelines [here](#).

The following resources related to this article are available online at www.sciencemag.org (this information is current as of July 9, 2015):

Updated information and services, including high-resolution figures, can be found in the online version of this article at:

<http://www.sciencemag.org/content/349/6244/171.full.html>

Supporting Online Material can be found at:

<http://www.sciencemag.org/content/suppl/2015/07/08/349.6244.171.DC1.html>

This article **cites 40 articles**, 7 of which can be accessed free:

<http://www.sciencemag.org/content/349/6244/171.full.html#ref-list-1>

This article appears in the following **subject collections**:

Physiology

<http://www.sciencemag.org/cgi/collection/physiology>